BEAM DIAGNOSTICS FOR COHERENT OPTICAL RADIATION INDUCED BY THE MICROBUNCHING INSTABILITY*

Alex H. Lumpkin#, Fermi National Accelerator Laboratory, Batavia, IL 60510, USA

Abstract
The observations of the microbunching instability were initially reported in S-band linacs that used photo-injected beams. However, we now have observations in linacs with thermionic cathode generated beams in the past year at SCSS, SACLA, and APS. A summary of the results is provided which also illustrate the beam diagnostics used.

INTRODUCTION

The generation of the ultra-bright beams required by modern free-electron lasers (FELs) has generally relied on chicane-based bunch compressions that often result in the microbunching instability [1, 2]. Following compression, spectral enhancements extend even into the visible wavelengths through the longitudinal space charge (LSC) impedances. Optical transition radiation (OTR) screens have been extensively used for transverse electron beam size measurements for the bright beams, but the presence of longitudinal microstructures (microbunching) in the electron beam or the leading edge spikes can result in strong, localized coherent enhancements (COTR) that mask the actual beam profile. We now have evidence for the effects in both rf photocathode (PC) gun injected linacs and thermionic-cathode (TC) gun injected linacs. Since the first observations, significant efforts have been made to characterize, model, and mitigate COTR effects on beam diagnostics [3-6]. An update on the state-of-the-art for diagnosing these effects will be given as illustrated by examples at LCLS, SCSS, SACLA, APS, and NLCTA. The most recent microbunching instability workshop was held in Pohang, Korea [7] in May 2013, and the website provides more details in the files for the talks including an extensive overview on observations [8].

INSTABILITY EFFECTS

It should be kept in mind that the modulation is even stronger in the several-micron-period regime where it impacts the effective energy spread and can reduce FELgain. As reference the original description by Saldin, Schneidmiller, and Yurkov [1] provides an analysis of the charge density noise being amplified via LSC impedances with the gain as a function of wavelength as shown in Fig. 1. In this case curve 1 includes energy spread as compared to curve 2 which is for a cold beam. Experimentally, one images the 0.4 to 0.7 µm regime of COTR with our standard CCD cameras in the various linac facilities. Another gain calculation has been given by Huang et al. [2] with maximum gain calculated at about 10 µm under an initial 150 µm period modulation with 8% amplitude.

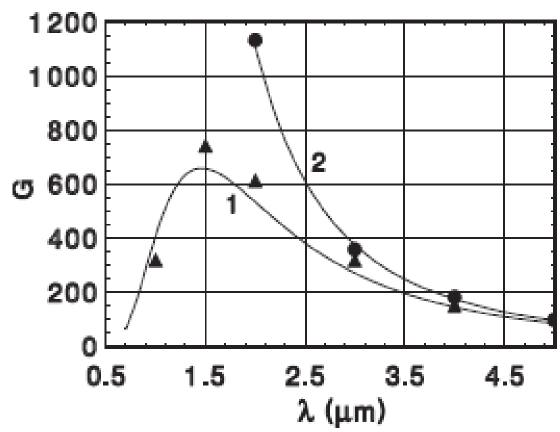

Figure 1: Calculated gain (G) for the microbunching instability versus wavelength from reference [1].

The instability effects were graphically demonstrated in the high energy spectra at LCLS as presented at FEL 10 by J. Welch [9]. The modulation in energy attributed to such microbunching is seen with the laser heater off in Fig. 2a, while it is suppressed with the laser heater on in Fig. 2b. Concomitantly, the observed x-ray spectra for the two cases showed the dramatic simplification of the spectrum with laser heater "on" in Fig. 3.

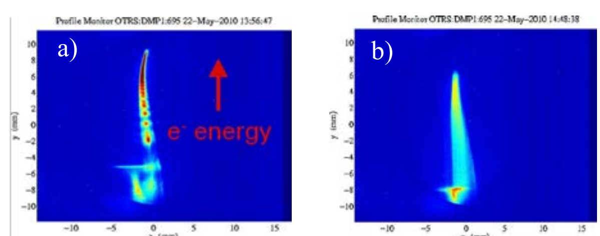

Figure 2: Examples of the LCLS electron beam high energy spectrum a) without and b) with the laser heater active [9].

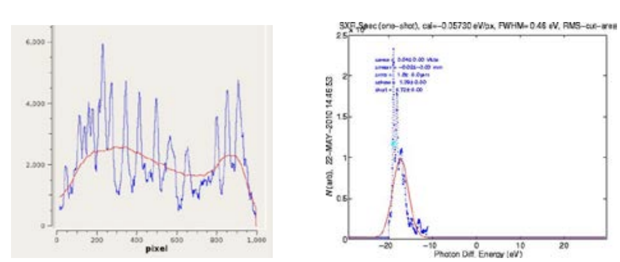

Figure 3: Corresponding x-ray spectra at LCLS for Fig. 2 without (left) and with (right) the laser heater active [9].

lumpkin@fnal.gov
*Work supported under Contract No. DE-AC02-07CH11359 with the United States Department of Energy.

ISBN 978-3-95450-126-7

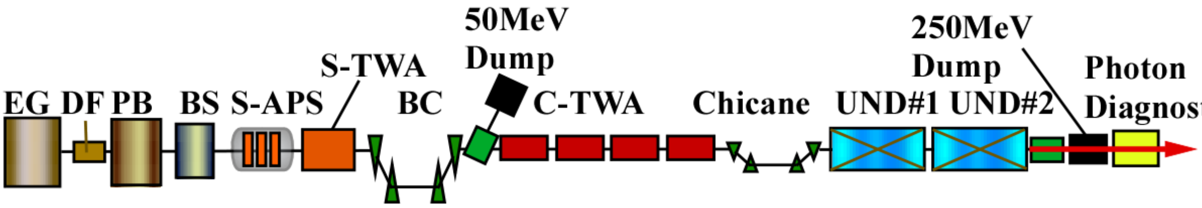

Figure 4: Schematic of the injector for the SCSS facility showing TC DC gun, accelerators, FEL, and beamlines. (courtesy of K. Togawa)

THERMIONIC CATHODE GUN BEAMS

One of the major developments in the past year involves the observations of the COTR effects attributed to the microbunching instability in TC gun beams, in both DC and rf guns. Example results are provided in this section.

SCSS Results

The SCSS linac is based on a DC TC gun with deflector, subharmonic bunchers, a S -band accelerator section, a ch icane bunch compressor, a C -band accelerator and another chicane for filtering the dark current beam as shown in Fig. 4 [10]. Using the second chicane as a b unch compressor was suggested in discussions at the μBI-4 workshop and following the FEL12 conference as well as looking for OTR enhancements at the station after this chicane. The experiments were initiated in October 2012 and were immediately successful. An example image is shown in Fig. 5 with about 250 pC micropulse charge, and the plot of OTR intensity in such images versus C-band phase setting is shown in Fig. 6. The intensity doubles at the -10 degrees off-crest phase point, and the fluctuations of the intensity dramatically increase compared to those at -5 and -15 degrees. This increase is attributed to a coherent process starting from noise in the beam due to the LSC microbunching instability, and the second compression shifted the effects into the visible light regime where they were sensed by the CCD camera. In the previous tests they had observed the OTR *before* this second chicane and with the C-band accelerator run on crest so no COTR effects were observed.

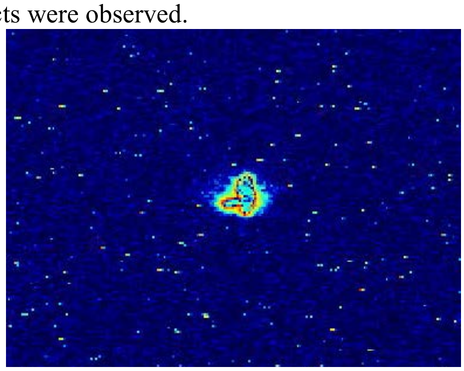

Figure 5: Image of the OTR and COTR generated at the beam profile station after the second bunch compressor at SCSS [11]. The x and y axes cover 4 x 3 mm.

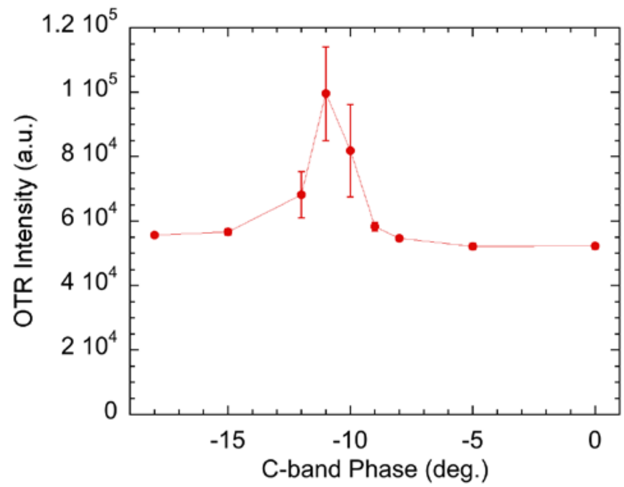

Figure 6: Plot of the C-band phase dependence of the OTR from the station after the second chicane at SCSS [11].

SACLA Results

The SACLA accelerator injector shown in Fig. 7 is based on the SCSS design with a few modifications such as the C-band correcting cavity. It also uses a DC TC gun with a deflector to select a part of the beam that is then subharmonically bunched. There are then three chicane-based compression stages with further acceleration to 1.4 GeV. After the third chicane bunch compression, they encountered significant COTR enhancements that saturated their CCD cameras [12]. To mitigate this effect they used spatial filtering with a scintillator crystal to obtain beam images. However, in the last year the staff revisited the stations to quantify the effects per suggestions from the Microbunching Instability Workshop 2012 attendees.

SACLA staff now report that the enhancement, or gain, is about 6000 over OTR [11], and they also showed the characteristic gradient-operator-related doughnut shape in the near field beam image in Fig. 8 as described by Loos et al. previously in the LCLS COTR images [4]. Additionally, they reported the enhanced red wavelength regime with intensity modulated spectrum in Fig. 9 as identified in the earlier APS/ANL PC rf gun based linac studies [13].

ISBN 978-3-95450-126-7

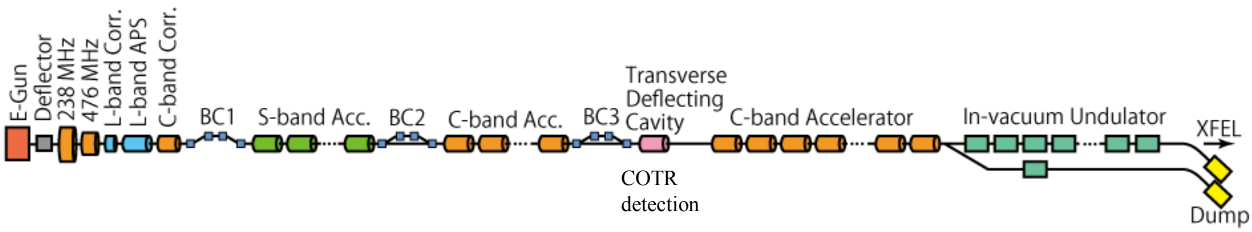

Figure 7: Schematic of the SACLA beamline with DC gun, bunchers, and accelerators with three chicanes for bunch com-presson. (courtesy of K. Togawa).

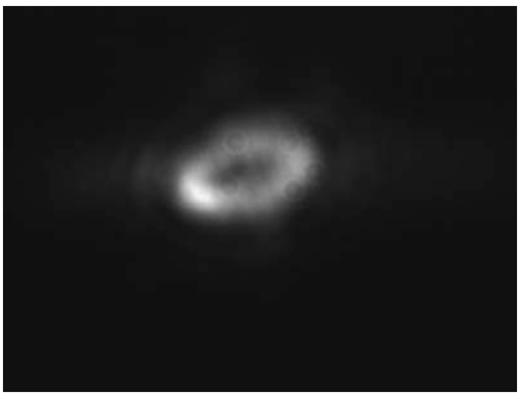

Figure 8: Beam image at 1.4 GeV after the third chicane at SACLA showing the COTR halo in the near field [11].

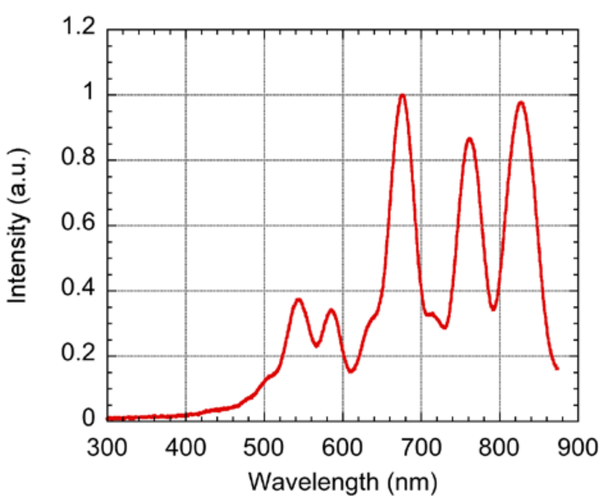

Figure 9: COTR spectrum obtained at 1.4 GeV after the third chicane at SACLA [11].

APS/ANL RESULTS

The initial experiments at ANL were on the PC rf gun beam, and the first look at the TC rf gun beam was also done. At that time the signature of COTR spiking in the beam profiles was only seen in the PC rf gun OTR images [5]. However, because the TC rf gun beam involves a set of 25 micropulses at the S-band frequency, the statistical fluctuations of COTR might be averaged out in the CCD camera integration. More recent tests show the increase in the integrated profiles when the compression in the chicane occurs following implementation of energy chirp in the beam entering the chicane. As shown in Fig. 10, two different horizontal profiles from 10-image sums were taken without (black and green circles) and with chicane compression (blue and red circles). The intensity of the profile peaks increased by >4 when operating at the rf phase that peaked the FIR coherent transition radiation (CTR) signal in the Golay cell after the chicane [7]. The alpha magnet did provide an initial compression of about ten prior to the chicane's factor of two compression. The charge transport at the end of the linac was tracked at 2 nC ±10% during the acquisition of these sets of images.

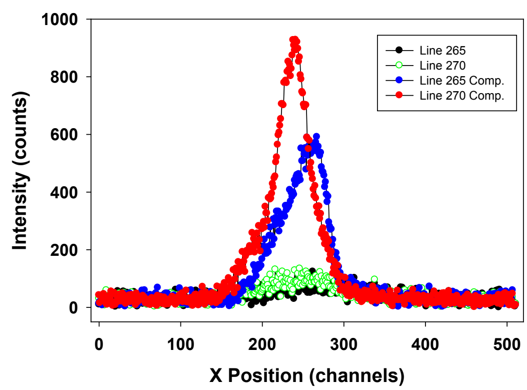

Figure 10: Profiles at lines 265 and 270 through the OTR sum images from TC rf gun beam uncompressed and compressed with a final beam energy of 325 MeV at APS.

NLCTA X-band RESULTS

Another interesting piece of the puzzle involves the observation of COTR with only 20-pC of charge in the micropulse following two chicane compressions at NLCTA as shown in Fig. 11. This facility has an S-band PC rf gun with two X-band accelerator sections that produce the 120-MeV beams [14]. Additionally, coherent optical undulator radiation has been reported [15].

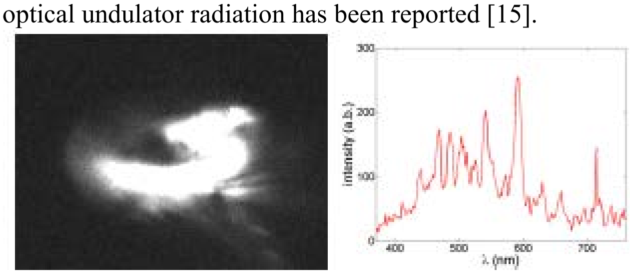

Figure 11: Typical COTR image (left) and wavelength spectrum following double compression at NLCTA [14].

ISBN 978-3-95450-126-7

Table 1: Summary of the COTR Effects Observed in Various Accelerator Facilities Including the Gun Type, Linac Energy, and Number of Chicanes or Compressions

Facility	Gun	Linac, Energy	Chicanes	COTR Effects
LCLS	PC, S-band	S-band, 250, 14 GeV	two	very strong, $x10^4$
APS	PC, S-band rf TC, S-band	S-band, 150, 325 MeV	one alpha magnet, one	x10-100 localized x4 integral
DESY	PC, L-band	SCRF, L-band, 1.2 GeV, linearizer	two	x 10-100 localized
SACLA	TC, DC gated	S-band, C-band, 1.4 GeV	three	$>6x10^3$ after 3 compressions
SCSS	TC, DC gated	S-band , C-band, 250 MeV	two	x2, Observable after two compressions
NLCTA	PC, S-band	X-band, 120 MeV	two of four	x20 after two

DISCUSSION

Table 1 is a summary of the scope of the observations in the various linacs including LCLS, DESY, and NLCTA and with the new TC gun beam results at SCSS, SACLA, and APS. The role of compression factors is indicated where second compressions in SCSS and APS were needed to display the COTR effect in TC gun beams. It is noted that the final enhancement of 6000 in SACLA after three chicanes in the TC DC gun beam approaches the very large enhancements in LCLS after two chicane compressions of the PC rf gun beam. Also, it is noted the transverse normalized emittances vary from 6-10 mm mrad in APS and NLCTA beams while LCLS, DESY, SCSS, and SACLA beams have emittances at about 1 mm mrad or below. All cases above exhibit some COTR effects.

SUMMARY

In summary, the microbunching instability as detected through the generation of COTR has become worldwide in interest. The observations of the microbunching instability attributed to longitudinal space charge impedances and CSR effects has become a more general phenomenon with cases reported in L-band, S-band, C-band, and X-band accelerators and with beams generated by both PC rf guns and TC rf and DC guns. There is an opportunity for using this broader empirical data base to elucidate the effect via further modeling efforts. Modeling of the TC gun beams still seems to be needed since the slice energy spread may not be as well understood at this time. Mitigations in the diagnostics have been reported in several labs [5,6,12], and suppression of the instability itself has been ongoing with laser heaters and dispersive elements. Further investigations are encouraged.

ACKNOWLEDGMENTS

The author acknowledges: discussions with D. Dowell, Z. Huang, and H. Loos of SLAC; W. Fawley (LBNL); D. Rule (NSWC); and R. Fiorito (UMD); support from K.-J. Kim, R. Gerig, and H. Weerts of the Argonne Accelerator Institute; the collaborations on ANL linac tests of N. Sereno, J. Dooling, S. Pasky, Y. Li, and Y. Sun of ANL; the support of M.Wendt and N. Eddy of Fermilab; and the figures provided by K. Togawa (Riken,SPring-8) and S. Weathersby (NLCTA/SLAC).

REFERENCES

[1] E.L. Saldin, E.A. Schneidmiller, and M.V. Yurkov, Nucl. Instr. and Methods, A490, 1 (2002).
[2] Z. Huang, M.Borland, P.Emma, J.Wu, C.Limborg, G. Stupakov, and J.Welch, Phys. Rev. ST-AB 7, 077701 (2004).
[3] D. Dowell et al., Proc. of FEL07, WEAAU01, JACoW.org.
[4] H. Loos et al., Proc. of FEL08, THBAU01, JACoW.org.
[5] A.H. Lumpkin et al., Phys. Rev. ST-AB **12**, 080702 (2009).
[6] C. Behrens et al., Phys. Rev. ST-AB **15**, 062801 (2012).
[7] Fifth Microbunching Instability Workshop, Pohang, Korea, Co-Chairs J.-H. Han, and K.-J. Kim, May 8-10, 2013.
[8] Alex H. Lumpkin, "Overview and Issues of Experimental Observation of Microbunching Instabilities", *ibid*.
[9] J. J. Welch, "X-ray Diagnostics Commissioning at LCLS", Talk presented at FEL10, FROAI1 (2010).
[10] K. Togawa et al., Proc. of the Fourth Microbunching Instability Workshop, Univ. of Maryland, April 11-13 2012.
[11] K. Togawa et al., Proc. of the Fifth Microbunching Instability Workshop, Pohang, Korea, May 8-10, 2013.
[12] H. Tanaka, Proc. of IPAC11, MOYCA01, 21, JACoW.org.
[13] A. H. Lumpkin et al., Proc. of FEL09, TUPC47, 352, JACoW.org.
[14] M. Dunning et al., Proc. of PAC11, MOP014, 130, JACoW. org.
[15] S. Weathersby et al., Proc. of PAC11, THP170, 2426, JACoW.org.

ISBN 978-3-95450-126-7